



ELSEVIER

Available online at www.sciencedirect.com
jmr&t
 Journal of Materials Research and Technology
journal homepage: www.elsevier.com/locate/jmrt

Synergistic effect of PTB emulsion, CaCO₃ whisker and Nano-SiO₂ on the properties of cement-based materials

Chunyu Zhang ^{a,c}, Meng Wang ^{a,c}, Xiuhan Li ^{a,c}, Rentai Liu ^{a,c,*}, Jia Yan ^{a,c},
 Zhijing Zhu ^{a,c}, Mengjun Chen ^{b,c,**}

^a School of Civil Engineering, Shandong University, Jinan 250061, Shandong, PR China

^b School of Qilu Transportation, Shandong University, Jinan 250003, Shandong, PR China

^c Geotechnical and Structural Engineering Research Center, Shandong University, Jinan 250061, Shandong, PR China

ARTICLE INFO

Article history:

Received 7 August 2023

Accepted 25 September 2023

Available online 29 September 2023

Keywords:

Synergistic effect

PTB emulsion

CaCO₃ whisker

Nano-SiO₂

Mechanical property

Micro-structure

ABSTRACT

With the rapid development of the civil engineering industry, performance requirements for building materials are also increasing rapidly. It is particularly critical to improve the performance of cement-based materials using admixtures. In this study, the synergistic effect of PTB (COMPAKTUNA.PRO) emulsion, calcium carbonate whisker (CaCO₃ whisker) and nano-silica (nano-SiO₂) on material properties was analyzed. Macroscopic properties such as rheology, compressive strength, flexural strength, durability, bond strength, and permeable pressure were tested. Microstructures were analyzed using the porosity, hydration heat, X-ray diffraction, and scanning electron microscopy methods. The results revealed that the PTB emulsion, CaCO₃ whiskers, and nano-SiO₂ increased the plastic viscosity and yield stress of the cement. When the nano-SiO₂ content was high, the fluidity of the slurry decreased significantly. Overall, PTB emulsion, CaCO₃ whisker and nano-SiO₂ can improve the strength, durability, bond strength, and permeability of composite materials. PTB emulsions can prolong the hydration process, resulting in low early strength and reduced compressive strength. However, they play a key role in terms of improving durability, bond strength, and permeability pressure. CaCO₃ whiskers yield slight improvements in various properties. Nano-SiO₂ can promote the hydration rate and hydration effect, thereby improving the strength, compactness, and properties of composite materials. Performance can be optimized by leveraging these synergistic effects and each material has its own unique advantages and limitations. In engineering applications, critical properties should be considered when selecting appropriate admixture contents. This study aimed to improve various properties and to develop materials that are suitable for the complex environment of underground engineering.

© 2023 The Author(s). Published by Elsevier B.V. This is an open access article under the CC BY-NC-ND license (<http://creativecommons.org/licenses/by-nc-nd/4.0/>).

* Corresponding author. School of Civil Engineering, Shandong University, Jinan 250061, Shandong, PR China.

** Corresponding author. School of Qilu Transportation, Shandong University, Jinan 250003, Shandong, PR China.

E-mail addresses: rentailiu@sdu.edu.cn (R. Liu), mjun@sdu.edu.cn (M. Chen).

1. Introduction

Concrete is widely used as a building material. However, concrete materials exhibit high brittleness, low tensile strength, and poor crack resistance [1,2], and the performance requirements for building materials have increased with the rapid development of the civil engineering industry [3,4]. In particular, the concrete structures of operational tunnels are prone to damage under the effects of the external environment. Many structures need to be repaired and as a result, maintenance materials have been widely developed [5,6]. To adapt to complex underground engineering environments, improving the working performance, durability, bonding performance, and impermeability of maintenance materials has become a major research focus. These properties can be improved by optimizing the contents of concrete admixtures [7–9].

Polymer emulsions, calcium carbonate whiskers (CaCO_3 whiskers) and nano-silica (nano- SiO_2) have become research hotspots [10–12]. Polymer emulsions are commonly used to modify cement-based materials [13–15]. High-molecular-weight polymers in a polymer emulsion can combine with cement matrices to increase cohesion and improve the toughness of cement-based materials [16,17]. By forming a continuous polymer film in a cement-based material, a polymer emulsion can effectively prevent the penetration of water, resulting in excellent impermeability [18,19]. Such polymers can also interact with the surfaces of other materials to form strong bonding forces, which improves the interfacial adhesion between cement matrices and other materials [20,21]. Cement-based materials modified with CaCO_3 whiskers represent a new research field [22,23]. Initial results indicate that the high strength and rigidity of CaCO_3 whiskers can increase the mechanical strength of concrete, including compressive, tensile, and bending strengths [24,25]. CaCO_3 whiskers have a slender shape and high tensile strength, allowing them to provide a bridging effect in a cement matrix, which resists the expansion of cracks, and improves cracking resistance and durability [26,27]. The addition of CaCO_3 whiskers can increase compactness and reduce porosity and micro-cracking, thereby improving impermeability [28]. Nano- SiO_2 has also been widely used in the modification of cement-based materials [29,30]. Nano- SiO_2 has a large specific surface area and high activity, and can react with hydration products to form uniform and dense cementitious material structures, which can improve the mechanical strength of cement-based materials [31–33]. Nano- SiO_2 can also fill pores and micro-cracks in cement matrices, and reduce the possibility of water penetration, which can improve impermeability and durability [34–36].

Research progress on modified cement-based materials has been rapid and many meaningful results have been achieved. However, each modified material has its own unique advantages and limitations. For example, polymer emulsions can significantly improve bond strength and impermeability, but reduce compressive strength. Nano- SiO_2 can significantly improve compressive strength, but reduces slurry fluidity. Polymer emulsions, CaCO_3 whiskers, and nano- SiO_2 are the research hotspots as cement-based modified materials. Studying the synergistic effect between polymer emulsions, CaCO_3

whiskers, and nano- SiO_2 can achieve the advantages of composite materials and overcome the disadvantages of a single component. Currently, few studies have analyzed the synergistic effect between polymer emulsions, CaCO_3 whiskers and nano- SiO_2 on material properties. The synergistic effect between three additives on the properties of composite materials are relatively unknown. It is important and innovative to carry out relevant research. Potential synergistic effect can promote multi-functional optimization, render them more suitable for complex underground engineering environments, and drive innovation in engineering applications. Therefore, it is both practical and innovative to conduct relevant studies in this area.

In this study, the synergistic effects of PTB emulsions, CaCO_3 whiskers, and nano- SiO_2 on various properties were analyzed. The individual and synergistic effects of these three admixtures on macroscopic properties were determined based on rheological properties, compressive strength, flexural strength, durability, bond strength, and permeable pressure tests. Microscopic mechanisms were studied using porosity and hydration heat tests, X-ray diffraction (XRD), and scanning electron microscopy (SEM). The positive and negative effects of the three admixtures on various properties were analyzed and the results provide theoretical support for performance evaluation and optimal ratio selection.

2. Experimental program

2.1. Materials and mixing proportions

Ordinary Portland cement following the Chinese standard GB 175-2007 produced by Jinan Shanshui Cement Co., Ltd. was used in our experiments. The physicochemical characteristics of this cement are listed in Table 1. PTB emulsions, CaCO_3 whiskers, and nano- SiO_2 were considered as additives to improve the properties of cement-based materials. The chemical name of the PTB emulsion is vinyl chloride-ethylene-vinyl ester terpolymer. It was obtained from Belgium Fine Chemicals Holdings Co., Ltd. The primary technical parameters are listed in Table 2. The CaCO_3 whiskers were obtained from Zhejiang Juyuan Chemical Co., Ltd. Nano- SiO_2 was obtained from Shandong Yousuo Chemical Co., Ltd. The particle characteristics of the CaCO_3 whiskers and nano- SiO_2 are listed in Table 3. Fig. 1 presents macroscopic and microscopic images of the PTB emulsion, CaCO_3 whiskers, and nano- SiO_2 . A powdery polycarboxylate superplasticizer produced by Shandong Hongxiang Construction Co., Ltd was also used. Tap water was used for cement mixing in this study.

In this study, 39 groups of samples with different mixing proportions were designed with sample S-1 as the control group, four groups of samples with different PTB emulsion contents (S-2 to S-5), five groups of samples with different CaCO_3 whisker contents (S-6 to S-10), five groups of samples with different nano- SiO_2 contents (S-11 to S-15), and samples with mixed dosages (S-16 to 39). The water-to-cement ratio was 0.5, which included the moisture content in the PTB emulsion. An appropriate proportion of superplasticizer was added. The mixing proportions are listed in Table 4. The goal of this study was to investigate the effects of PTB emulsions, CaCO_3 whiskers, and nano- SiO_2 on the properties of cement-based materials under

Table 1 – Physicochemical properties of the cement used in this study.

Cement	Initial setting time (min)	Final setting time (min)	Flexural strength (28 d) (MPa)	Compressive strength (28 d) (MPa)
P.O 42.5	>150	<240	>6.5	>42.5

Table 2 – Main technical parameters of the PTB emulsion.

Appearance	Solubility	Viscosity (mPa·s)	Solid solution Content (%)	MFT (°C)	Density (g/cm ³)	PH
Milky white emulsion	Fully soluble in water	80 ± 20	50 ± 1	7	1.12 ± 0.01	7–9

Note: MFT is the minimum film formation temperature.

Table 3 – Particle characteristics of CaCO₃ whisker and nano-SiO₂.

Materials	Particle size	Specific surface	Shape
CaCO ₃ whisker	Length: 20–80 μm; Diameter: 1–2 μm	/	Needle bar granular
Nano-SiO ₂	20 nm	240 m ² /g	Sphere

both individual and composite conditions. The content ranges of the PTB emulsion, CaCO₃ whiskers, and nano-SiO₂ used in this study were determined based on the content ranges of existing references and our previous results.

2.2. Test procedures

2.2.1. Rheological testing

An RST-SST Rheometer produced by Brookfield was used for rheological testing (see Fig. 2). This rheometer consists of a data monitoring system, temperature control system, rotor, and vertical cylinder. Rheological parameters were tested using the rotation measurement method. The selected CCT-40 rotor had a length of 60 mm and diameter of 40 mm. The temperature control and monitoring module utilizes a circulating water temperature control. The raw materials were weighed according to the mixing proportions listed in Table 3. A homogenous slurry was obtained by stirring the solution at 200 rpm for 5 min. A shear rate of 200 s⁻¹ was applied for 60 s and then the shear rate was varied uniformly from 0 to 1000 s⁻¹. The temperature was controlled at 20 °C throughout the testing process, and shear stress and shear rate curves were obtained.

2.2.2. Compressive strength and flexural strength testing

Compressive and flexural strengths were tested according to the GB/T 17671-2021 standard. The test instrument was an SANS microcomputer electronic pressure testing machine manufactured by the Meisite Company and specimens with dimensions of 40 mm × 40 mm and 40 mm × 40 mm × 160 mm were used for compressive and flexural strength tests, respectively. The loading speed was 2 mm/min in the compressive strength tests and 0.5 mm/min in the flexural strength tests. The compressive and flexural strengths were tested following standard curing (20 °C and 95% RH) for 3 and 28 d, respectively.

The calculation formula for compressive strength R_c is presented in Eq. (1).

$$R_c = \frac{F_c}{A} \quad (1)$$

Here, F_c is the peak load (N) during compression failure and A is the area of the compression zone (mm²).

The calculation formula for flexural strength R_f is presented in Eq. (2).

$$R_f = 1.5 \times \frac{F_f L}{b h^2} \quad (2)$$

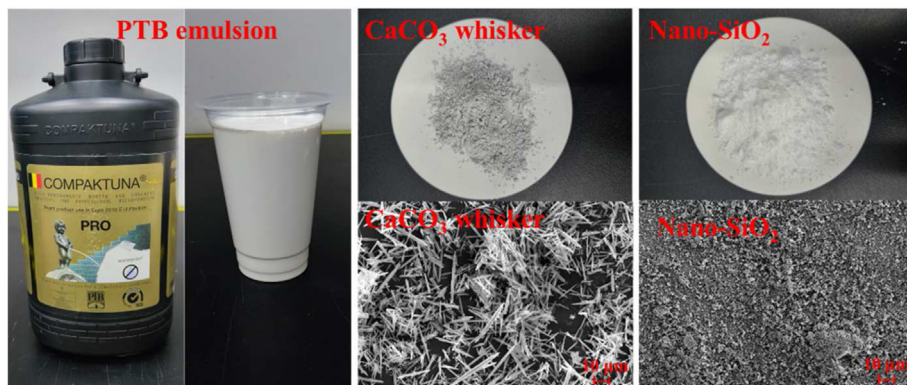


Fig. 1 – Macroscopic and microscopic images of the PTB emulsion, CaCO₃ whisker and nano-SiO₂.

Table 4 – Mixing proportions of the composite materials.

Sample number	Cement (kg/m ³)	Water (kg/m ³)	PTB emulsion (kg/m ³)	CaCO ₃ whisker (kg/m ³)	Nano-SiO ₂ (kg/m ³)	Superplasticizer (%)
S-1	1000	500	0	0	0	1.5
S-2	1000	480	40	0	0	1.5
S-3	1000	460	80	0	0	1.5
S-4	1000	440	120	0	0	1.5
S-5	1000	420	160	0	0	1.5
S-6	990	500	0	10	0	1.5
S-7	980	500	0	20	0	1.5
S-8	970	500	0	30	0	1.5
S-9	960	500	0	40	0	1.5
S-10	950	500	0	50	0	1.5
S-11	990	500	0	0	10	1.5
S-12	980	500	0	0	20	1.5
S-13	970	500	0	0	30	1.5
S-14	960	500	0	0	40	1.5
S-15	950	500	0	0	50	1.5
S-16	990	460	80	0	10	1.5
S-17	990	460	80	10	0	1.5
S-18	970	460	80	0	30	1.5
S-19	970	460	80	10	20	1.5
S-20	970	460	80	20	10	1.5
S-21	970	460	80	30	0	1.5
S-22	950	460	80	0	50	1.5
S-23	950	460	80	10	40	1.5
S-24	950	460	80	20	30	1.5
S-25	950	460	80	30	20	1.5
S-26	950	460	80	40	10	1.5
S-27	950	460	80	50	0	1.5
S-28	990	420	160	0	10	1.5
S-29	990	420	160	10	0	1.5
S-30	970	420	160	0	30	1.5
S-31	970	420	160	10	20	1.5
S-32	970	420	160	20	10	1.5
S-33	970	420	160	30	0	1.5
S-34	950	420	160	0	50	1.5
S-35	950	420	160	10	40	1.5
S-36	950	420	160	20	30	1.5
S-37	950	420	160	30	20	1.5
S-38	950	420	160	40	10	1.5
S-39	950	420	160	50	0	1.5

Note: Bold is the samples used below for durability and hydration analysis.

Here, F_f is the peak load (N) at fracture failure, L is the distance between the supporting cylinders (mm), b is the specimen width (mm), and h is the specimen height (mm).

2.2.3. Durability testing

Durability was analyzed through freeze-thaw cycles and dry-wet cycles. A TDR-5 freeze-thaw cycle testing machine was used for freeze-thaw cycle testing. An LSY-18 concrete dry-wet cycle testing machine was used for dry-wet cycle testing. The dry-wet cycle and freeze-thaw cycle tests used cuboid specimens with dimensions of 40 × 40 × 160 mm. After 28 d of standard curing (20 °C and 95% RH), compressive strength was tested following 50 dry-wet cycles and 100 freeze-thaw cycles. The loss ratio of the compressive strength was calculated using Eq. (3).

$$N = \frac{R_{c-28} - R_{c-n}}{R_{c-28}} \times 100\% \quad (3)$$

Here, N is the loss ratio of the compressive strength (%), R_{c-28} is the compressive strength (MPa) after 28 d, and R_{c-n} is the compressive strength (MPa) following n dry-wet and freeze-thaw cycles.

2.2.4. Bond strength testing

Bond strength was measured using an SANS microcomputer electronic pressure testing machine. First, standard mortar samples with dimensions of 40 × 40 × 80 mm were prepared. The cement/standard sand/water ratio was 1:3:0.5. The surface of the mortar was treated to render it rough and uniform. The treated specimens were placed in a 40 mm × 40 mm × 160 mm mold and the remaining half of the mold was filled with a composite material. The composite materials consisted of samples with different PTB emulsion contents, CaCO₃ whisker contents, nano-SiO₂ contents, and mixed dosages. The influences of different mixing proportions on the bond strength varied. After the specimens were demolded, the bond strength

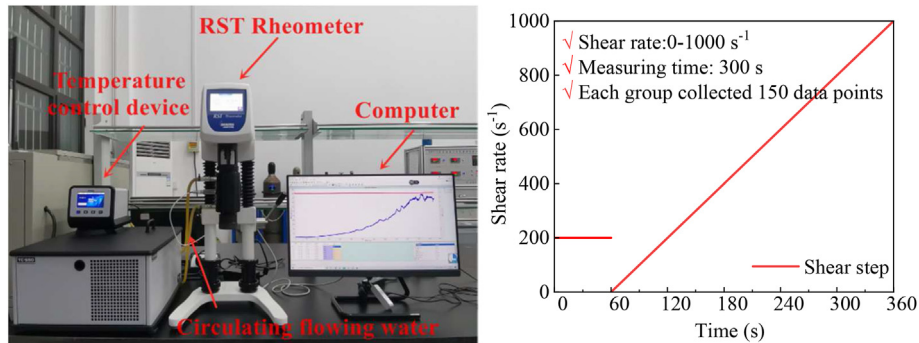


Fig. 2 – RST-SST Rheometer and testing program.

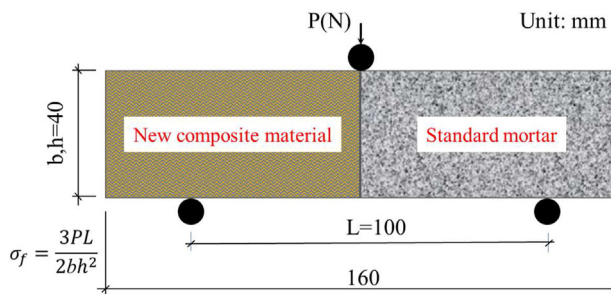


Fig. 3 – Sample structure for bond strength testing.

was tested after standard curing for 28 d. A bonding specimen consisting of standard mortar and a composite material is illustrated in Fig. 3. Bond strength tests were conducted in accordance with the Chinese standard JC/T 2357-2019. There are various methods for testing the bond strength between repairing material and concrete structure. In this paper, the testing method of interfacial flexural tensile strength was referred in part 7.6 of standard JC/T 2357-2019.

2.2.5. Permeable pressure testing

Permeable pressure was tested according to the industrial standard JGJ/T70-2009. An SS-15 mortar permeameter was used to test round table samples with dimensions of $\varphi 70$ mm \times $\varphi 80$ mm \times 30 mm. In the permeable pressure tests, the pressure started from 0.2 MPa and increased to 0.3 MPa after maintaining a constant pressure for 2 h, and then

increased by 0.1 MPa every 1 h. When water seepage occurred on the surfaces of the specimens, the test was stopped and the pressure was recorded. The permeable pressure value was calculated based on the maximum stress among four specimens in each group of six specimens without water seepage, as shown in Eq. (4).

$$P = H - 0.1 \quad (4)$$

Here, P is the permeable pressure (MPa) and H is the water pressure when water seepage occurred in the specimens.

2.2.6. Porosity testing

In this study, the nuclear magnetic resonance method was used to test porosity, which is simple, convenient, and does not cause damage to samples. Cubic specimens with dimensions of 40 mm \times 40 mm \times 40 mm were used and porosity was tested after 28 d of standard curing. A low-field nuclear magnetic resonance analyzer (MacroMR12-150V-I, see Fig. 4) was used for these tests. To measure porosity accurately, a vacuum-pressure saturation device was used to saturate the samples before testing. The number of hydrogen atoms in the pore water was measured using NMR to calculate porosity based on nuclear magnetic resonance.

2.2.7. Hydration heat testing

The heat flow of hydration was tested using an isothermal calorimeter (I-Cal 8000 HPC; see Fig. 5). This high-precision isothermal calorimeter utilized eight test channels. Each sample contained 50 g of cementitious material, and the



Fig. 4 – Nuclear magnetic resonance instrument (MacroMR12-150V-I).



Fig. 5 – Isothermal calorimeter (I-Cal 8000 HPC).

cementitious material and water were stirred evenly in a 125 ml sample cup. Each sample cup was then placed in the corresponding channel. Heat flow (Watts), heat flow per gram (W/g), heat (Joules), and heat per gram (J/g) were monitored. The heat flow and heat of hydration were tested over 7 d in this experiment.

2.2.8. Microstructure characterization

Microstructures were observed and analyzed using a Thermo Fisher 250 Environmental Scanning Electron Microscope. Phase identification of the hydration products was performed using a Malvern Panalytical Aeris X-ray Diffractometer. Data were collected between 20 angles of 5° and 90°, and the step size was 0.02°. The step time was maintained at 2 s. Following the mechanical strength tests, samples were selected and subjected to microscopic testing.

A summary of the tests, and the numbers and sizes of the specimens are provided in [Table 5](#).

3. Results and discussion

3.1. Rheological properties

The Bingham model and Herschel-Bulkley model are widely accepted models for describing the rheological properties of cement-based fluids [37,38]. In this study, rheological parameters were fitted and rheological properties were analyzed using the Bingham and Herschel-Bulkley models.

Bingham model:

$$\tau = \tau_0 + \mu \cdot \gamma \quad (5)$$

Herschel-Bulkley model:

$$\tau = \tau_0 + K \cdot \gamma^n \quad (6)$$

Here, τ is the shear stress (Pa), γ is the shear rate (s^{-1}), τ_0 is the yield stress (Pa), μ is the plastic viscosity ($Pa \cdot s$), K is the consistency coefficient ($Pa \cdot sn$), and n is the rheological index.

Based on the relationship between the shear stress and shear rate ($\tau-\gamma$), the fitting curve and fitting function of Bingham model and Herschel-Bulkley model were established (see [Figs. 6 and 7](#)). [Table 6](#) presents the fitting functions and correlation coefficients (R^2) based on the Bingham and Herschel-Bulkley models. With increasing PTB emulsion content (S-1 to S-5), the shear stress increases at a given shear rate. With increasing $CaCO_3$ whisker content (S-1 and S-6 to S-10), the shear stress increases at a given shear rate. The addition of the PTB emulsion and $CaCO_3$ whiskers did not change the rheological properties and the rheological curves were similar. However, as the dosage changed, the rheological parameters also changed. The Bingham and Herschel-Bulkley models can accurately fit slurries with different PTB emulsion and $CaCO_3$ whisker contents, and the correlation coefficients (R^2) all exceed 97%.

The Bingham model can fit slurries containing 1% and 2% nano- SiO_2 , whereas the Herschel-Bulkley model can fit slurries containing 1%, 2%, and 3% nano- SiO_2 . When the nano- SiO_2 content exceeds 3%, the rheological curves do not

Table 5 – Summary of the tests used, and size and number of specimens.

Test method	Specimen size	Specimen number
Rheological test	Slurry	Three specimens per mix ratio
Compressive strength	40 × 40 × 40 mm ³	Three specimens per mix ratio
Flexural strength	40 × 40 × 160 mm ³	Three specimens per mix ratio
Durability	40 × 40 × 160 mm ³	Three specimens per mix ratio
Bond strength	40 × 40 × 160 mm ³	Three specimens per mix ratio
Permeable pressure	φ70 × φ80 × h30 mm ³	Three specimens per mix ratio
Porosity	40 × 40 × 40 mm ³	Three specimens per mix ratio
Hydration heat	Slurry	Three specimens per mix ratio
SEM test	less than 1 cm ³	Three points per specimen
XRD test	Power	One specimen per mix ratio

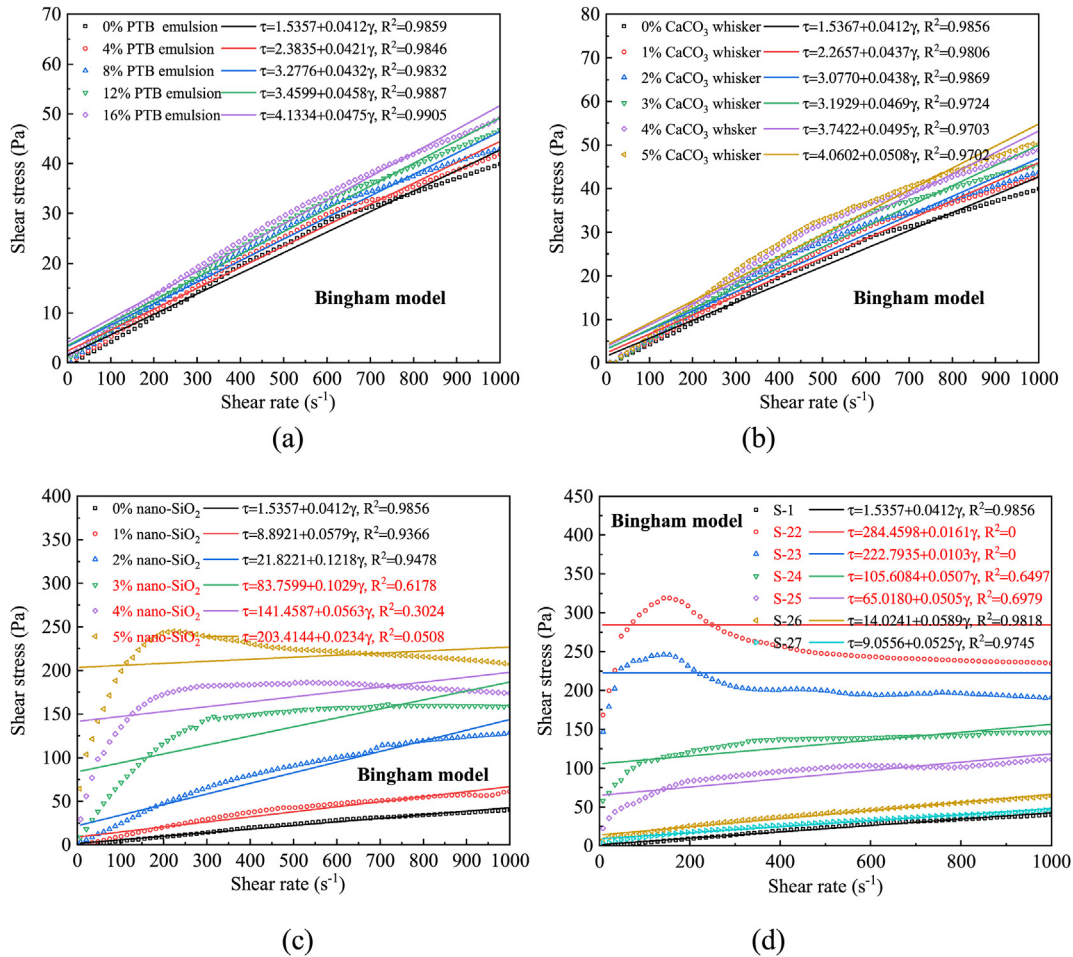


Fig. 6 – Fitting curves of the Bingham model: (a) different PTB emulsion contents, (b) different CaCO₃ whisker contents, (c) different nano-SiO₂ contents, and (d) mixed dosages.

conform to the traditional rheological model of cement slurry. This indicates that the addition of nano-SiO₂ to a slurry significantly affects the shear rate. The addition of nano-SiO₂ also changes the rheological curve. When the nano-SiO₂ content exceeds 3%, the rheological curve cannot be fitted using the Bingham and Herschel-Bulkley models. For the mixed-dose samples (S-22–S-27), both rheological models can be used to fit the slurry when the nano-SiO₂ content is low. When the nano-SiO₂ content is high, it does not conform to either of the rheological models. Overall, the influence of nano-SiO₂ on the rheological properties is greater than that of the PTB and CaCO₃ whiskers.

Figs. 8 and 9 present the yield stress and plastic viscosity, respectively, obtained using the Bingham model. With an increase in PTB emulsion content, the yield stress increases from 1.5357 to 4.1334 Pa and the plastic viscosity increases from 0.0412 to 0.0475 Pa s. With an increase in CaCO₃ whisker content, the yield stress increases from 1.5357 to 4.0602 Pa and the plastic viscosity increases from 0.0412 to 0.0508 Pa s. With an increase in nano-SiO₂ content, the plastic viscosity and yield stress both increase. When the nano-SiO₂ content exceeds 3%, the rheological curves do not conform to the Bingham model and the fitted data deviate from the actual values.

The yield stress values obtained by the Herschel-Bulkley model are relatively small and could not be analyzed. Additionally, the plastic viscosity could not be obtained based on the parameter definitions.

Fig. 10 presents the rheological indexes (*n*) obtained using the Herschel-Bulkley model. When *n* > 1, the slurry exhibited shear thickening. When *n* < 1, the slurry exhibited shear thinning. The greater the deviation of the rheological index from one, the greater the degree of shear thickening or thinning [39,40]. The rheological indexes for different mixing proportions were all less than one, indicating shear thinning. With increasing PTB emulsion content, the rheological index decreased from 0.8505 to 0.7891. With increasing CaCO₃ whisker content, the rheological index decreased from 0.8505 to 0.7809. With an increase in nano-SiO₂ content, the rheological index significantly decreased from 0.8505 to 0.0845. For mixed-dosage samples (S-22 to S-27), the rheological index was mainly affected by nano-SiO₂ content. Analysis of the rheological index revealed that the slurry containing nano-SiO₂ was most significantly affected by the shear rate.

By combining the changes in the rheological curves, yield strength, plastic viscosity, and rheological index, it can be concluded that nano-SiO₂ has the greatest impact on

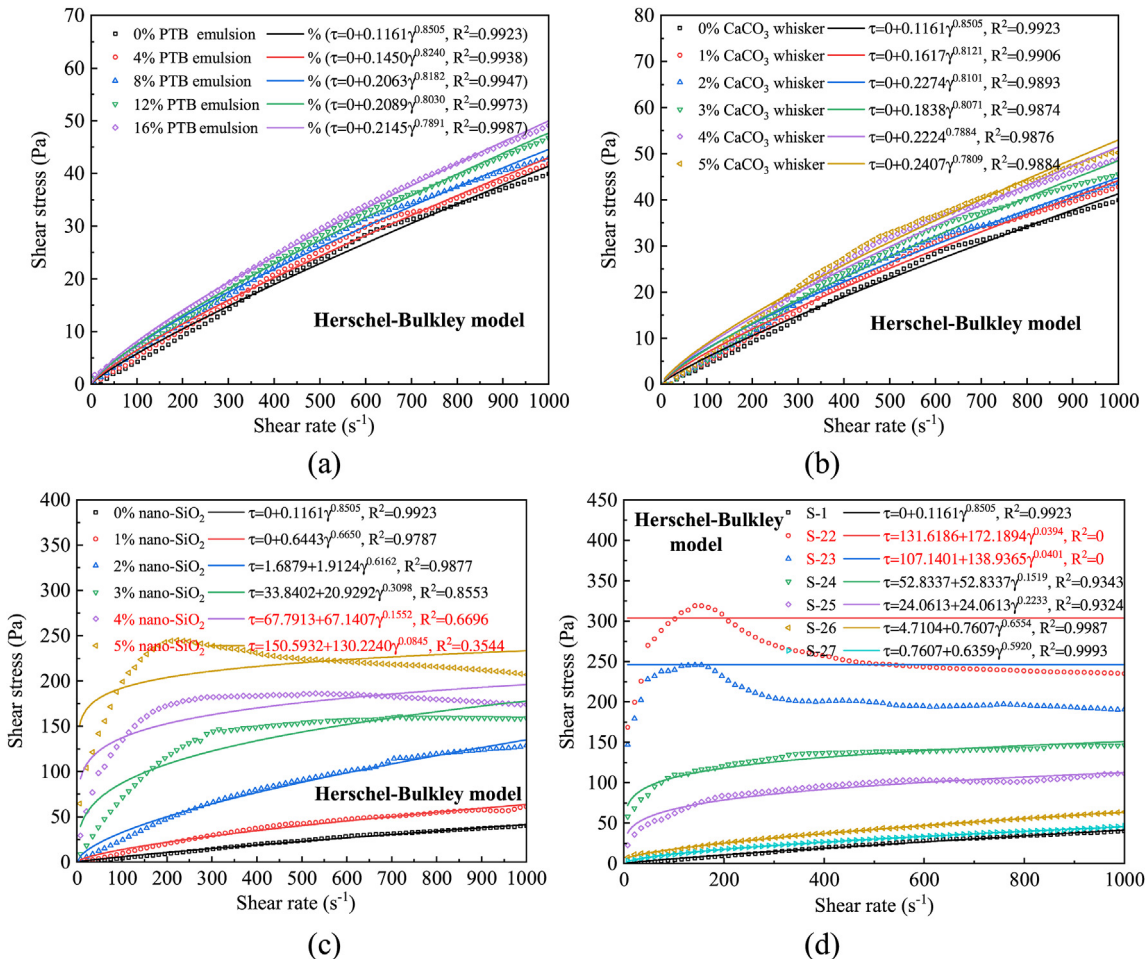


Fig. 7 – Fitting curves of the Herschel-Bulkley model: (a) different PTB emulsion contents, (b) different CaCO₃ whisker contents, (c) different nano-SiO₂ contents, and (d) mixed dosages.

rheological parameters. PTB emulsion and CaCO₃ whiskers have little effect on rheological parameters. The polymer chains in PTB emulsions interact with cement particles or other hydration products in the slurry, leading to the extension and cross-connection of polymer chains, thereby forming a network structure. This network structure can effectively hinder the flow of particles and increase viscosity [41,42]. The slender morphology of CaCO₃ whiskers hinders the relative motion between particles, which impedes internal flow and increases viscosity [43]. For samples containing nano-SiO₂, sodium dodecyl benzene sulfonate was added as a dispersant to water. They were stirred on a magnetic stirrer for 2 min to fully dissolve the dispersant. Then, nano-SiO₂ was slowly added and magnetically stirred for 2 min. The stirred dispersion was placed in an ultrasonic disperser and sonicated for 10 min. Finally, the nano-SiO₂ dispersion was added to the cement powder and stirred evenly. The nano-SiO₂ dispersion method produces small particles that are more evenly dispersed in the cement slurry. This allows nano-SiO₂ to come into more complete contact with the other components in the

slurry. Additionally, nano-SiO₂ also has surface activity and reacts with water molecules and other products. These characteristics can increase intermolecular interactions, thereby reducing the fluidity of the slurry [44,45]. The large specific surface area and small particle size of nano-SiO₂ facilitates the formation of a network structure in the slurry. This network structure hinders the movement of particles, thereby leading to an increase in viscosity. However, this network is easily broken at high shear rates. Therefore, slurries containing nano-SiO₂ are significantly affected by the shear rate [46]. When the content of nano-SiO₂ is high, the rheological curve does not conform to the traditional Bingham and Herschel-Bulkley models. Nano-SiO₂ significantly affects the rheological properties. The PTB emulsion and CaCO₃ whiskers can slightly increase yield strength and plastic viscosity. Under the synergistic effect, the rheological properties are mainly affected by the content of nano-SiO₂. When selecting admixture contents to improve comprehensive properties of materials, particularly nano-SiO₂, rheological properties should be carefully considered as they have an important effect on

Table 6 – Fitting models and correlation coefficients (R^2).

Sample number	Bingham model		Herschel-Bulkley model	
	$\tau = \tau_0 + \mu \cdot \gamma$	R^2	$\tau = \tau_0 + K \cdot \gamma^n$	R^2
S-1	$\tau = 1.5357 + 0.0412\gamma$	0.9855	$\tau = 0 + 0.1161\gamma^{0.8505}$	0.9923
S-2	$\tau = 2.3835 + 0.0421\gamma$	0.9846	$\tau = 0 + 0.1450\gamma^{0.8240}$	0.9955
S-3	$\tau = 3.2776 + 0.0432\gamma$	0.9832	$\tau = 0 + 0.2063\gamma^{0.8182}$	0.9972
S-4	$\tau = 3.4599 + 0.0458\gamma$	0.9887	$\tau = 0 + 0.2089\gamma^{0.8030}$	0.9964
S-5	$\tau = 4.1334 + 0.0475\gamma$	0.905	$\tau = 0 + 0.2145\gamma^{0.7891}$	0.9982
S-6	$\tau = 2.2657 + 0.0437\gamma$	0.9806	$\tau = 0 + 0.1617\gamma^{0.8121}$	0.9906
S-7	$\tau = 3.0770 + 0.0438\gamma$	0.9869	$\tau = 0 + 0.2274\gamma^{0.8101}$	0.9893
S-8	$\tau = 3.1929 + 0.0469\gamma$	0.9724	$\tau = 0 + 0.1838\gamma^{0.8071}$	0.9874
S-9	$\tau = 3.7422 + 0.0495\gamma$	0.9703	$\tau = 0 + 0.2224\gamma^{0.7884}$	0.9876
S-10	$\tau = 4.0602 + 0.0508\gamma$	0.9702	$\tau = 0 + 0.2407\gamma^{0.7809}$	0.9884
S-11	$\tau = 8.8921 + 0.0579\gamma$	0.9366	$\tau = 0 + 0.6443\gamma^{0.6650}$	0.9787
S-12	$\tau = 21.8221 + 0.1218\gamma$	0.9478	$\tau = 1.6879 + 1.9124\gamma^{0.6162}$	0.9877
S-13	$\tau = 83.7599 + 0.1029\gamma$	0.6178	$\tau = 33.8402 + 20.9292\gamma^{0.3098}$	0.8553
S-14	$\tau = 141.4587 + 0.0563\gamma$	0.3024	$\tau = 67.7913 + 67.1407\gamma^{0.1552}$	0.6696
S-15	$\tau = 203.4144 + 0.0234\gamma$	0.0508	$\tau = 150.5932 + 130.2240\gamma^{0.0845}$	0.3544
S-22	$\tau = 284.4598 + 0.0161\gamma$	0	$\tau = 131.6186 + 172.1894\gamma^{0.0394}$	0
S-23	$\tau = 222.7935 + 0.0103\gamma$	0	$\tau = 107.1401 + 138.9365\gamma^{0.0401}$	0
S-24	$\tau = 105.6084 + 0.0507\gamma$	0.6497	$\tau = 52.8337 + 52.8337\gamma^{0.1519}$	0.9343
S-25	$\tau = 65.0180 + 0.0505\gamma$	0.6979	$\tau = 24.0613 + 24.0613\gamma^{0.2233}$	0.9324
S-26	$\tau = 14.0241 + 0.0589\gamma$	0.9818	$\tau = 4.7104 + 0.7607\gamma^{0.5920}$	0.9987
S-27	$\tau = 9.0556 + 0.0525\gamma$	0.9745	$\tau = 0.7607 + 0.6359\gamma^{0.6554}$	0.9993

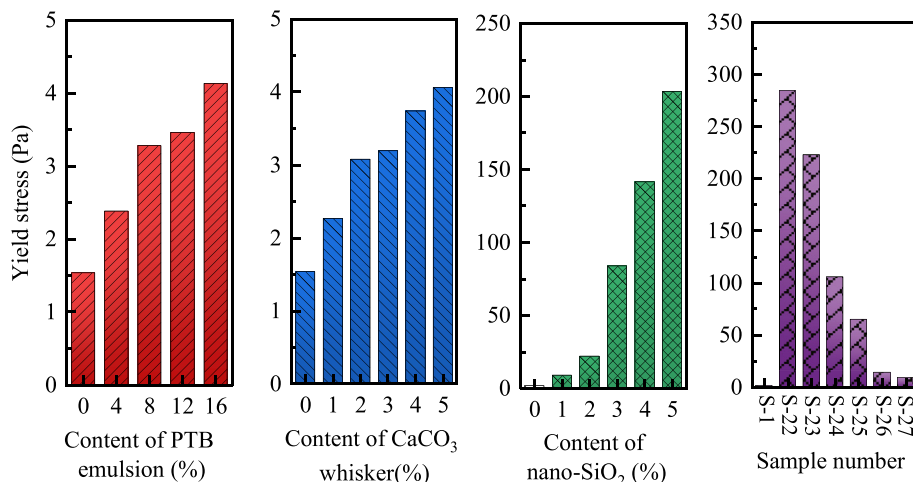
Note: The correlation coefficient of these data (Italics) is low after fitting.

pumping performance, stability, and flow. Although nano-SiO₂ has significant improvement in other performance, the content should be selected in an appropriate range.

3.2. Compressive strength and flexural strength

Figs. 11–14 present the compressive and flexural strengths with different PTB emulsion contents, CaCO₃ whisker contents, nano-SiO₂ contents, and mixed dosages in order. With an increase in PTB emulsion content, the compressive strengths at 3 d and 28 d do not exhibit a significant increasing or decreasing trend. However, the compressive strength of the samples containing the PTB emulsion was lower than that of

the control sample S-1. With an increase in the PTB emulsion content, the 3 d flexural strength increased from 4.414 to 5.586 MPa and the 28 d flexural strength increases from 6.107 to 7.212 MPa. With an increase in CaCO₃ whisker content, the 3 d compressive strength increases from 20.401 to 24.833 MPa and the 28 d compressive strength increases from 42.779 to 49.253 MPa. The 3 d flexural strength increases from 4.414 to 5.745 MPa and the 28 d flexural strength increased from 6.107 to 7.518 MPa. With an increase in nano-SiO₂ content, the 3 d compressive strength increases from 20.401 to 28.343 MPa and the 28 d compressive strength increases from 42.779 to 52.125 MPa. The 3 d flexural strength increases from 4.414 to 6.557 MPa and the 28 d flexural strength increases from 6.107

**Fig. 8 – Yield Stress with different mixing proportions.**

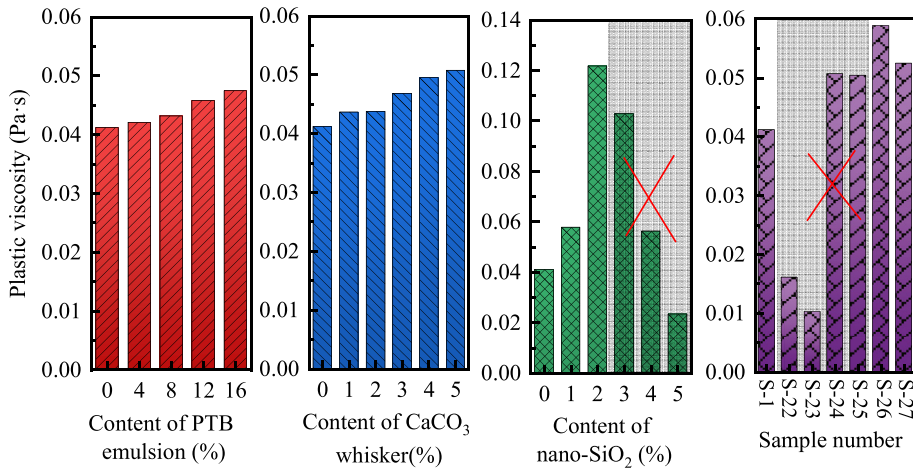


Fig. 9 – Plastic viscosity with different mixing proportions.

to 7.654 MPa. For the mixed-dosage samples, the compressive strengths of samples S-16, S-17, S-28, and S-29 with the PTB emulsion were lower than those of the control group S-1. This is because the PTB emulsion was added to samples S-16, S-17, S-28, and S-29, but the contents of CaCO₃ whiskers and nano-SiO₂ were low. Although the PTB emulsion was also added to the other samples, the contents of CaCO₃ whiskers and nano-SiO₂ were relatively high. As a result, the flexural and compressive strengths of the other samples were higher than those of the control group S-1.

In general, PTB emulsions can reduce compressive strength, but increase flexural strength. CaCO₃ whiskers and nano-SiO₂ can improve both flexural and compressive strengths. Nano-SiO₂ has the most significant impact in terms of improving flexural and compressive strengths. Under mixed-dosage conditions, the flexural and compressive strengths were generally higher than those of the control group with the compressive strengths of samples S-16, S-17, S-28, and S-29 being exceptions. The influence mechanisms of the PTB emulsion, CaCO₃ whiskers, and nano-SiO₂ on flexural and compressive strengths are different. A PTB emulsion is flexible and elastic. Compared to cement-based materials, it

exhibits greater deformation under pressure. This results in the polymer emulsion being unable to provide sufficient support or transfer pressure to the cement-based materials when subjected to compressive forces, thereby resulting in a reduction in compressive strength. Additionally, a PTB emulsion can prolong the hydration process, causing more of the water phase to be lost during curing, which also reduces compressive strength [47]. However, a polymer emulsion can form bonds with hydration products and an elastic film to improve the integrity of composite materials. The elasticity and ductility of polymer emulsions can also absorb and disperse stress, slow the development of cracks, and improve flexural strength [15]. CaCO₃ whiskers have high hardness and strength, and can fill micropores and defects. This increases the density and compactness of concrete, thereby improving its compressive strength. CaCO₃ whiskers also limit crack propagation through bridging, thereby improving toughness and flexural performance [48]. Nano-SiO₂ has an extremely small particle size and can fill micropores and defects. Through this filling effect, nano-SiO₂ can increase density and reduce porosity. Nano-SiO₂ can also react with hydration products to form cementitious substances, which can increase the amount of crystalline

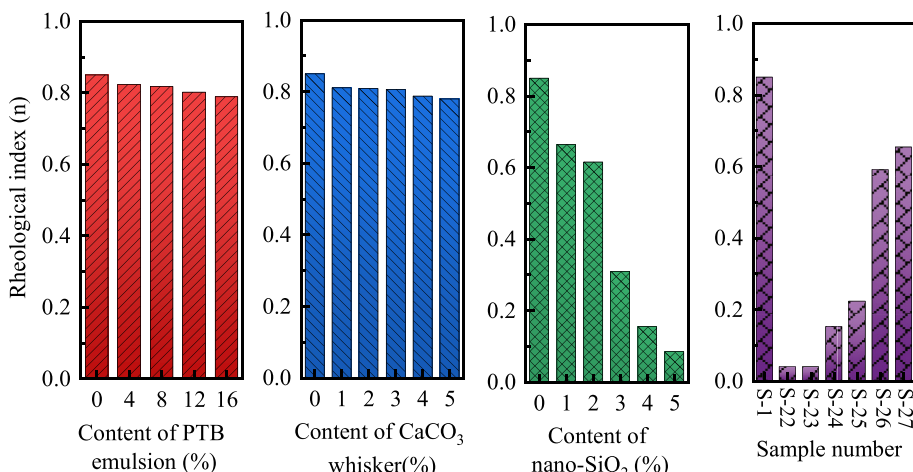


Fig. 10 – Rheological indexes (n) with different mixing proportions.

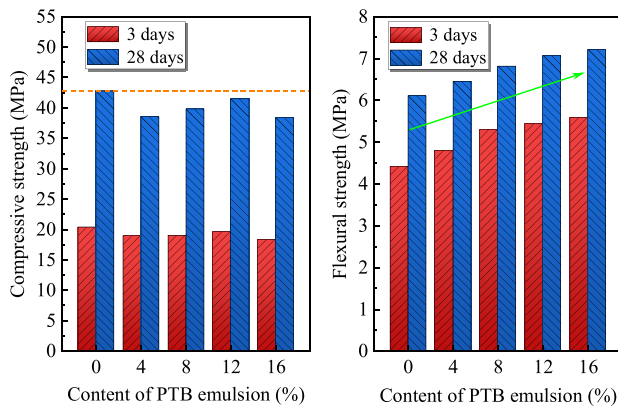


Fig. 11 – Compressive and flexural strengths with different PTB emulsion contents.

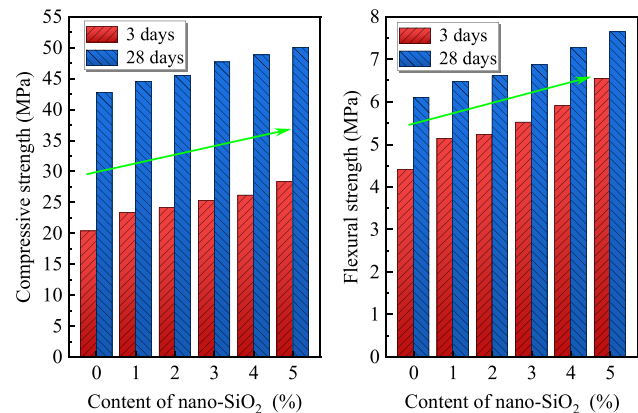


Fig. 13 – Compressive and flexural strengths with different nano-SiO₂ contents.

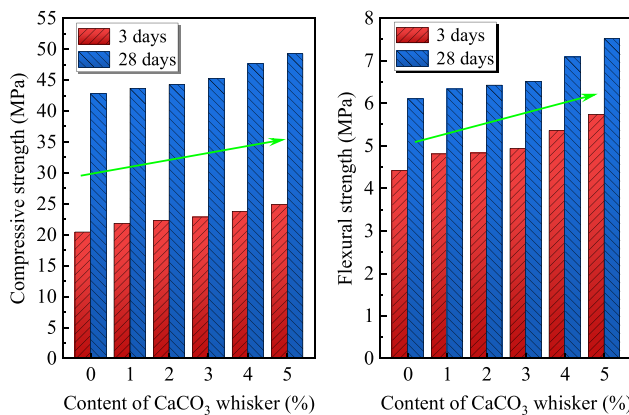


Fig. 12 – Compressive and flexural strengths with different CaCO₃ whisker contents.

substances and improve overall material strength [49]. The PTB emulsion reduced compressive strength and improved flexural strength, while the CaCO₃ whiskers and nano-SiO₂ improved both the flexural and compressive strengths. At mixed dosage, the compressive strength can be affected by three admixtures simultaneously. When the high content of PTB emulsion and low content of CaCO₃ whiskers and nano-SiO₂, the compressive strength will be lower than the control group S-1. When the high content of PTB emulsion and high content of CaCO₃ whiskers and nano-SiO₂, the compressive strength will be higher than the control group S-1. The compressive strength will change with the content of the three admixtures. Nano-SiO₂ has the most obvious effect on the increase of strength, and the PTB emulsion can reduce the compressive strength. Therefore, when PTB emulsion is added to improve other properties, the influence of PTB emulsion on compressive strength should be considered.

3.3. Durability

The control group S-1, and samples S-3, S-8, S-13, and S-25, which contained the PTB emulsion, CaCO₃ whiskers, nano-

SiO₂, and mixed dosages, respectively, were selected for durability analysis. The compressive strength and loss ratio of compressive strength are presented in Figs. 15 and 16, respectively. After 50 freeze-thaw cycles, the compressive strengths of S-1, S-3, S-8, S-13, and S-25 decreased by 7.486, 5.810, 7.424, 7.258, and 5.879 MPa, respectively. After 100 freeze-thaw cycles, the compressive strengths of S-1, S-3, S-8, S-13, and S-25 decreased by 9.625, 7.442, 9.189, 9.359, and 7.620 MPa, respectively. After 50 dry-wet cycles, the compressive strengths of S-1, S-3, S-8, S-13, and S-25 decreased by 6.845, 4.776, 6.790, 6.207, and 10.982 MPa, respectively. After 100 dry-wet cycles, the compressive strengths of S-1, S-3, S-8, S-13, and S-25 decreased by 11.133, 8.755, 10.864, 10.982, and 9.145 MPa, respectively.

Compared to the control group S-1, the PTB emulsion, CaCO₃ whiskers, nano-SiO₂, and mixed dosages improved durability overall. The loss ratios of the samples with the PTB emulsion were the lowest. The effect of the PTB emulsion in terms of improving durability was the most obvious. A polymer emulsion can form a flexible polymer membrane that can prevent water penetration and reduce water absorption, thereby improving the durability of cement-based materials [50,51]. When micro-damage occurs in cement-based materials, CaCO₃ whiskers recrystallize in the damaged area, fill cracks, and restore integrity and strength, which also improves the durability of cement-based materials [52]. Nano-SiO₂ can react with hydration products to form a dense structure, thereby improving both mechanical properties and durability [53,54]. In summary, PTB emulsions, CaCO₃ whiskers, nano-SiO₂ all can improve durability. Under the synergistic effect, the improvement degree of durability is affected by the ratio of the three admixtures. For example, the compressive strength loss rate of sample 2–25 is higher than that of S-3 but lower than that of samples S-8 and S-13. The improvement of durability is not a simple superposition of three admixtures, but the result of mutual influence. In order to significantly improve the durability, it is necessary to choose the best proportion. Meanwhile, content selection should focus on other properties.

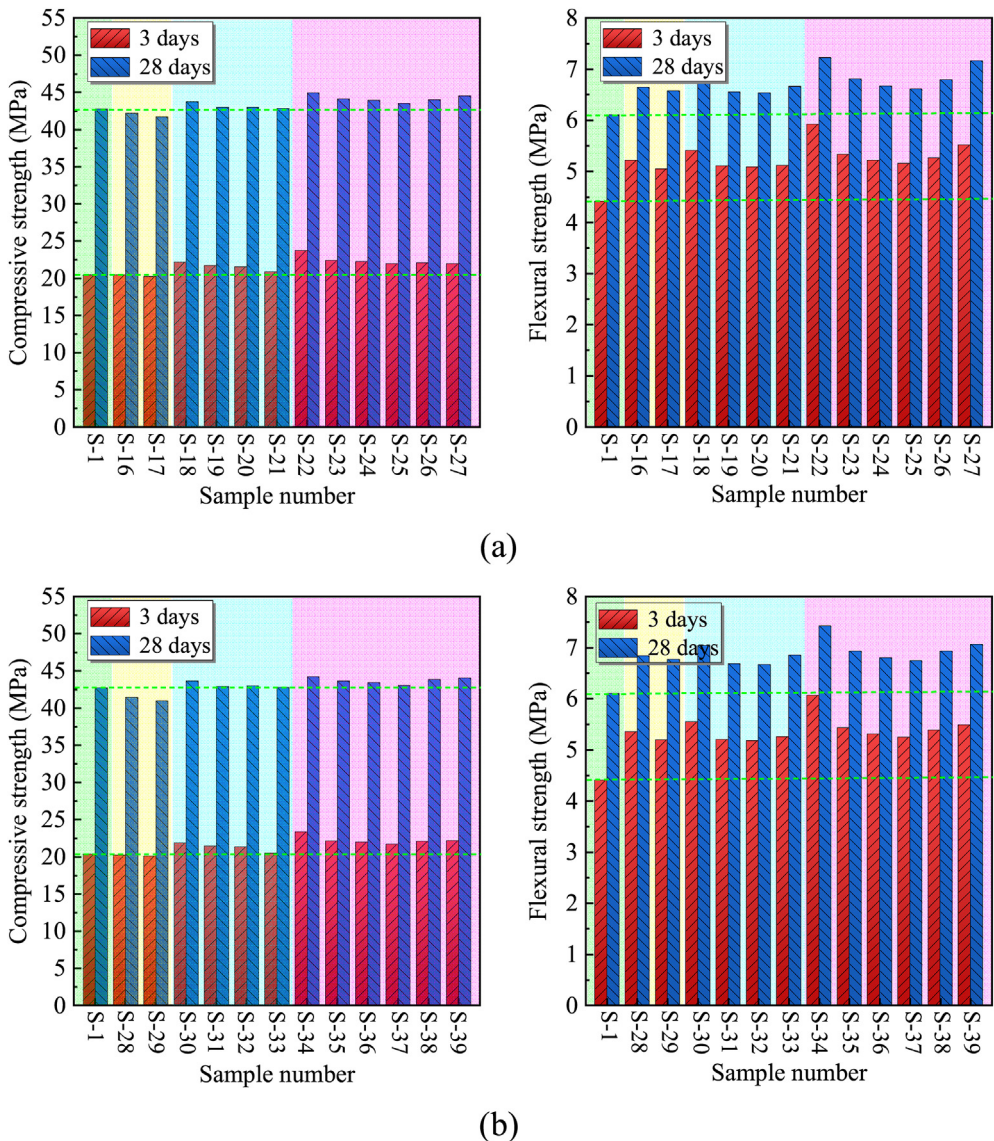


Fig. 14 – Compressive and flexural strengths with mixed dosages: (a) S16 to S27 and (b) S-28 to S-39.

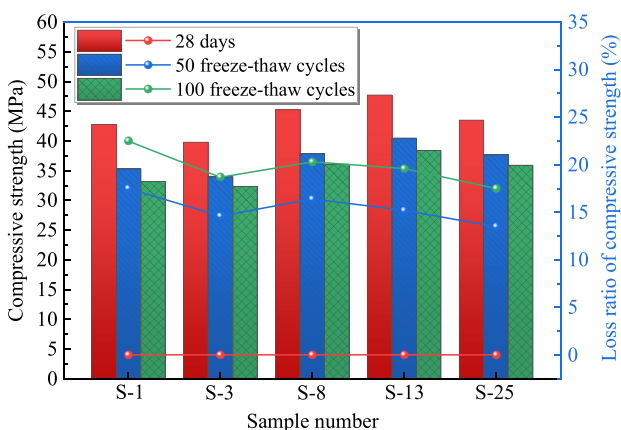


Fig. 15 – Compressive strengths and loss ratios of compressive strength after freeze-thaw cycles.

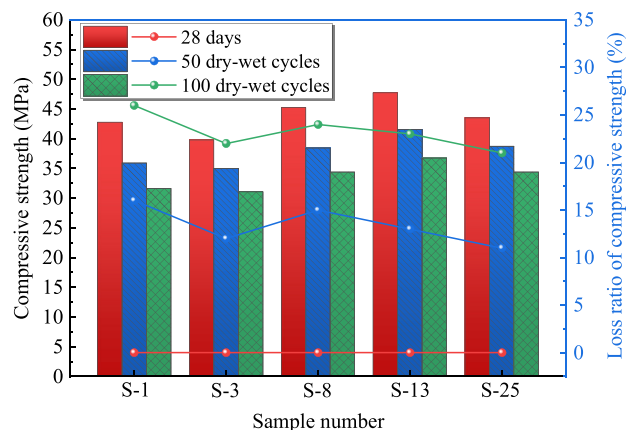


Fig. 16 – Compressive strengths and loss ratio of compressive strength after dry-wet cycles.

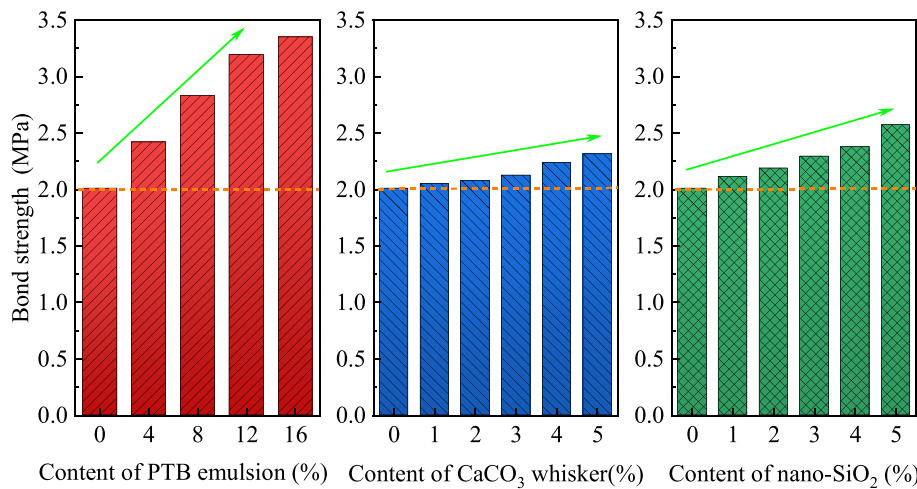


Fig. 17 – Bond strengths with different contents of the PTB emulsion, CaCO₃ whiskers, and nano-SiO₂.

3.4. Bond strength

The bond strengths of samples with different mixing proportions are presented in Figs. 17 and 18. With an increase in PTB emulsion content, the bond strength increases from 2.012 to 3.356 MPa. With an increase in CaCO₃ whisker content, the bond strength increases from 2.012 to 2.316 MPa. With an increase in nano-SiO₂ content, the bond strength increases from 2.012 MPa to 2.573 MPa. PTB emulsions can significantly increase the bond strength of composite materials. The effects of CaCO₃ whiskers and nano-SiO₂ in terms of increasing bond strength are less significant. For samples S-16 to S-39 with mixed dosages, the bond strengths were higher than that of the control group S-1. The bond strengths of the samples with 16% PTB emulsion content (S-28 to S-39) were generally higher than those of the samples with 8% PTB emulsion content (S-16 to S-27). The polymer particles in the PTB emulsion have small sizes, allowing them to fill micropores and cracks at contact interfaces. During the hydration process, water is gradually absorbed and evaporated, and the polymer particles also lose

water to form a film that is attached to the pore wall of the base mortar. This has the effect of filling and bridging, and increases the cohesion strength of the bond interface, thereby increasing overall bond strength [17,55]. PTB emulsions, CaCO₃ whiskers, nano-SiO₂ all can improve bond strength, but PTB emulsions play a major role in improving bond strength. Compared with a single admixture, the bond strength has been improved in different degrees under the synergistic effect. The content should be appropriate to achieve the best performance. PTB emulsion can greatly improve bond strength, but the influence on compressive strength should also be considered. A moderate amount of PTB emulsion with the right content of CaCO₃ whiskers and nano-SiO₂ may work better.

3.5. Permeable pressure

The permeable pressures of samples with different mixing proportions are presented in Figs. 19 and 20. With an increase in PTB emulsion content, the permeable pressure increases

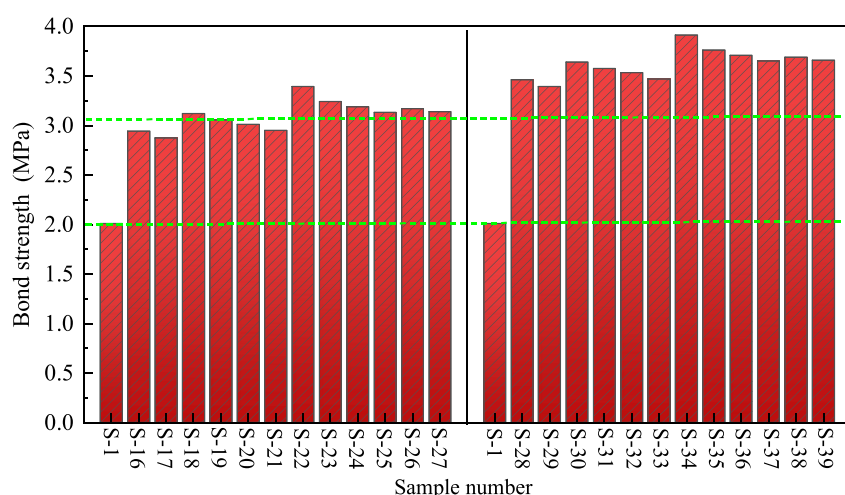


Fig. 18 – Bond strengths with mixed dosages.

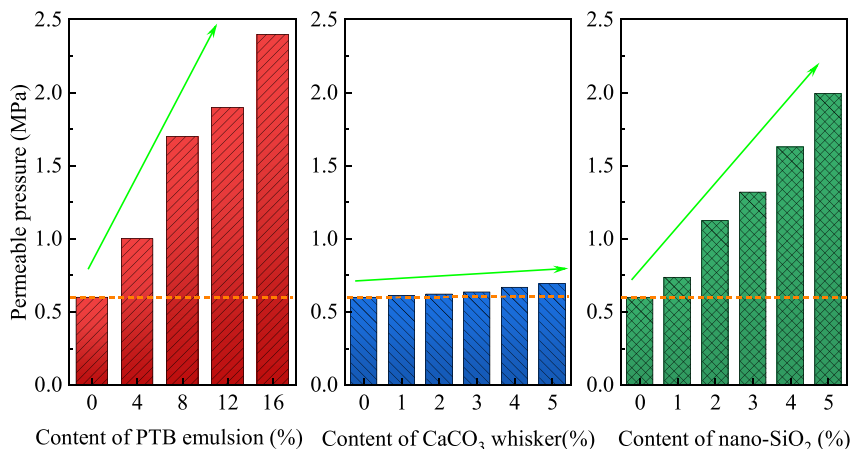


Fig. 19 – Permeable pressures with different contents of PTB emulsion, CaCO_3 whiskers, and nano- SiO_2 .

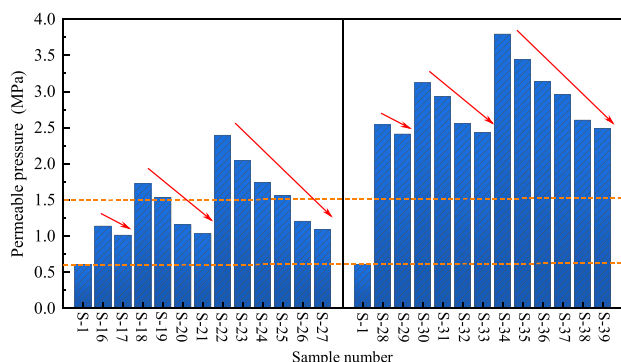


Fig. 20 – Permeable pressures with mixed dosages.

from 0.6 to 2.4 MPa. With an increase in CaCO_3 whisker content, the permeable pressure increases from 0.6 to 0.7 MPa. With an increase in nano- SiO_2 content, the permeable pressure increases from 0.6 to 2.0 MPa. The PTB emulsion and nano- SiO_2 significantly increase the permeability pressure, whereas the CaCO_3 whiskers have no significant effect. For samples S-16 to S-39 with mixed dosages, the permeable pressures are higher than those of the control group S-1.

Additionally, the permeable pressures of the samples with 16% PTB emulsion content (S-28 to S-39) are generally higher than those of the samples with 8% PTB emulsion content (S-16 to S-27). For a given PTB emulsion content, the permeable pressure decreases with decreasing nano-SiO₂ content and increasing CaCO₃ whisker content. This also indicates that the PTB emulsion and nano-SiO₂ increase the permeable pressure. The polymer particles in the PTB emulsion form a polymer membrane in the cement-based materials. This reduces the number of penetration paths for water and other permeating media, thereby improving the permeable pressure [56]. Nano-SiO₂ can fill micropores in cement-based materials. This improves density and reduces the number of penetration paths, thereby improving the permeable pressure [35,49]. PTB emulsions and nano-SiO₂ all can significantly improve permeable pressure. The improvement effect of CaCO₃ whiskers is not obvious. Under the synergistic effect, the permeable pressure of the samples is higher than that of the control group S-1. When the content of PTB emulsion and nano-SiO₂ is high, the improvement effect of permeable pressure is more obvious. Meanwhile, the influence of PTB emulsion and nano-SiO₂ on compressive strength and rheology should be considered.

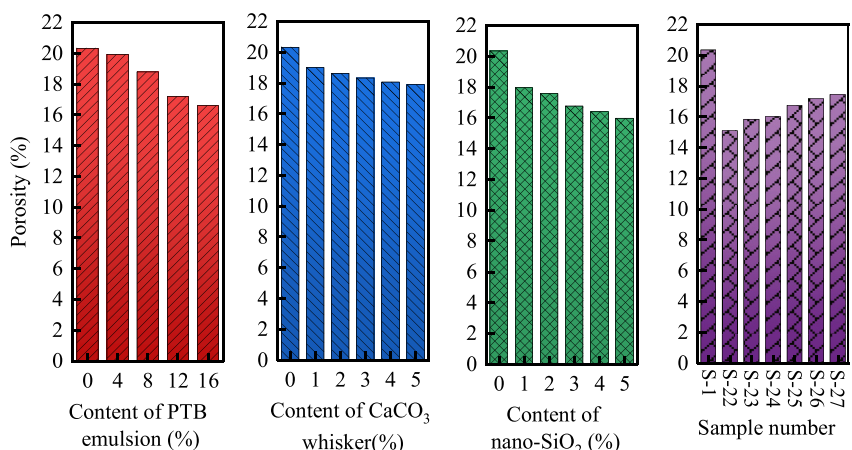


Fig. 21 – Porosities with different contents of PTB emulsion, CaCO₃ whiskers, and nano-SiO₂, and mixed dosages.

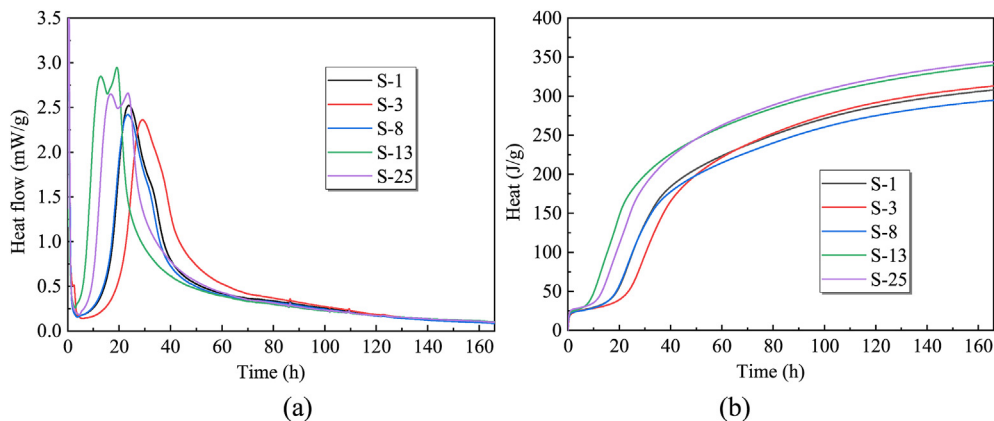


Fig. 22 – Heat flow and Heat with different mixing proportions: (a) Heat flow; (b) Heat.

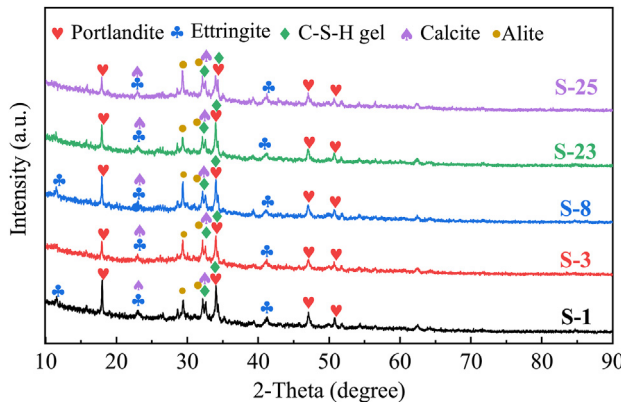


Fig. 23 – XRD results for hydration products with different mixing proportions.

3.6. Analysis of microscopic mechanisms

The results of porosity analysis are presented in Fig. 21. With an increase in PTB emulsion content, the porosity decreases from 20.350% to 16.596%. With an increase in CaCO_3 whisker content, the porosity decreases from 20.350% to 17.898%. With

an increase in nano- SiO_2 content, the porosity decreases from 20.350% to 15.985%. Nano- SiO_2 has the most significant effect in terms of reducing porosity. For samples S-22 to S-27 with mixed dosages, the porosity was lower than that of the control group S-1. PTB emulsions can reduce porosity, which is the main reason for the improved durability and permeable pressure observed with their addition. Nano- SiO_2 can also reduce porosity, which is the main reason for the improved compressive and flexural strength, durability, and permeable pressure observed with their addition.

The control group S-1, and the samples S-3, S-8, S-13, and S-25, which contained the PTB emulsion, CaCO_3 whiskers, nano- SiO_2 , and a mixed dosage, respectively, were selected to analyze hydration heat. The heat flows and heat levels at different mixing proportions are presented in Fig. 22. The early heat flow in S-3 was the lowest. The early heat flows in samples S-1 and S-8 were not significantly different. The early heat flows of samples S-13 and S-25 were the highest. The heat level of S-8 was the lowest. The heat levels of S-1 and S-3 were not significantly different. The heat levels of S-13 and S-25 are relatively high. It is evident that nano- SiO_2 can promote the hydration rate and hydration effect, thereby improving the strength and density of composite materials. The PTB emulsion has a negative impact on the early hydration rate

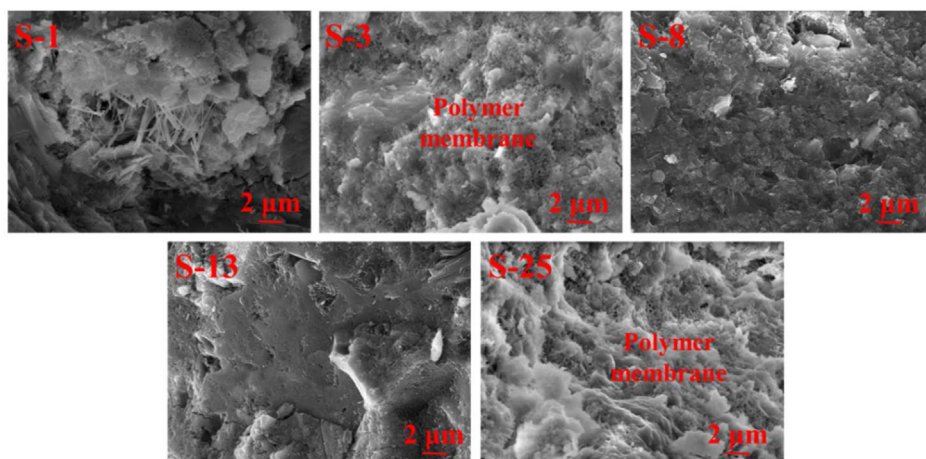


Fig. 24 – Microstructures of hydration products with different mixing proportions.

and extends the hydration process. This leads to a loss of the water phase, thereby reducing the compressive strength of composite materials. CaCO_3 whiskers can fill micropores and defects in materials, thereby improving their mechanical properties. However, this does not promote hydration.

The control group S-1, and the samples S-3, S-8, S-13, and S-25 were selected for microstructure analysis. The XRD patterns of the hydration products are presented in Fig. 23. The PTB emulsion, CaCO_3 whiskers, and nano- SiO_2 led to no significant changes in the hydration products and the main hydration products included portlandite, ethylite, C-S-H gel, Calcite, and Alite. These are consistent with the hydration products of ordinary Portland cement. The microstructures of the hydration products are presented in Fig. 24. In the control group S-1, discontinuous structures were observed between the hydration products and many pores, but there were few connections between pores. When the PTB emulsion was added (S-3 and S-25), a uniform and interconnected polymer mesh structure could be observed and this polymer mesh connected the hydration products. When CaCO_3 whiskers (S-8) and nano- SiO_2 (S-13) were added, the compactness increased significantly as a result of the filling effect and the number of pores was significantly reduced. PTB emulsions, CaCO_3 whiskers, and nano- SiO_2 can effectively change the microstructure of a cement mixture, leading to the observed improvements in compressive strength, durability, bond strength, and permeable pressure.

3.7. Limitations and future research

In this study, the effects of PTB emulsions, CaCO_3 whiskers, and nano- SiO_2 on the rheological properties, flexural and compressive strengths, durability, bond strength, and permeable pressure of concrete were analyzed. In particular, we analyzed performance changes under single-variable and mixed-dosage conditions, but did not perform an in-depth analysis of influence mechanisms. Specifically, under mixed-dosage conditions, it is not the superposition of individual variables, but the interaction mechanisms between the three admixtures lacking in-depth exploration. We analyzed the influence of three variables on the performance of cement paste, but their influence on mortar needs to be studied further in the future. This is the limitations of this study and the focus of the next study.

4. Conclusions

In this study, the synergistic effects of a PTB emulsion, CaCO_3 whiskers, and nano- SiO_2 on various properties of concrete were analyzed and the following conclusions were drawn.

- (1) The PTB emulsion and CaCO_3 whiskers increased yield strength and plastic viscosity, but did not change the rheological type of the cement slurry. The Bingham and Herschel-Bulkley models fit cement slurries with different PTB emulsion and CaCO_3 whisker contents well. Nano- SiO_2 increased the yield strength and plastic viscosity of the cement slurry. When the nano- SiO_2 content was greater than 3%, the slurry fluidity

decreased significantly and the rheological curves did not conform to the Bingham or Herschel-Bulkley models. Nano- SiO_2 significantly affected rheological properties and appropriate dosages of nano- SiO_2 should be selected for specific applications.

- (2) The PTB emulsion reduced compressive strength, but increased flexural strength, whereas CaCO_3 whiskers and nano- SiO_2 improved both compressive and flexural strengths. Therefore, appropriate dosages of PTB emulsion should be selected for specific applications.
- (3) PTB emulsions, CaCO_3 whiskers, and nano- SiO_2 can improve durability during dry-wet and freeze-thaw cycles. The compressive strength loss ratios of samples with added PTB emulsion were relatively small and the PTB emulsion had the most obvious effect in terms of improving durability. Under the synergistic effects of the three admixtures, the durability of a composite material was optimized.
- (4) PTB emulsions, CaCO_3 whiskers, and nano- SiO_2 improved the interfacial bond strength between composite materials and mortar. However, effects of CaCO_3 whiskers and nano- SiO_2 on bond strength were not obvious. The PTB emulsion increased the cohesion between the mortar and composite material, thereby significantly improving the bond strength. Under the synergistic effects of the three admixtures, the bond strength of a composite material was optimized.
- (5) PTB emulsions, CaCO_3 whiskers, and nano- SiO_2 all improve the permeability of composite materials, but the increase in the permeable pressure with the addition of CaCO_3 whiskers was not significant. The PTB emulsion and nano- SiO_2 significantly improved the permeable pressure. Again, the permeable pressure was optimized under the synergistic effects of the three admixtures.
- (6) CaCO_3 whiskers and nano- SiO_2 can reduce porosity, which is the main mechanism behind their improvement of the strength, durability, and permeability of composite materials. A PTB emulsion can form a polymer mesh to connect hydration products and cement particles, thereby effectively reducing porosity, which is the main mechanism behind its improvement of the durability and permeability of composite materials.
- (7) Nano- SiO_2 can increase the hydration rate and hydration effect to improve the strength and density of composite materials. However, nano- SiO_2 significantly reduced the fluidity of the cement slurry in this study. The PTB emulsion had a negative effect on the early hydration rate, resulting in low early strength, which should be considered in practical applications.
- (8) Nano- SiO_2 has a significant influence on rheology and can reduce the fluidity of cement slurry, but can significantly improve material strength and permeable pressure. PTB emulsion can reduce compressive strength, but is the main reason for an increase in bond strength and permeable pressure. CaCO_3 whiskers can increase material strength, bond strength, permeable pressure and durability. However, the promotion effect of CaCO_3 whiskers is not as obvious as PTB emulsion and nano- SiO_2 . Considering the comprehensive properties of materials, a single admixture can't achieve the

best properties. Material performance is optimized under the synergistic effects of multiple admixtures. The main properties can be improved by adding PTB emulsions and nano-SiO₂. Owing to the influence of PTB emulsion and nano-SiO₂ on compressive strength and rheology, the content should not be too high. An appropriate amount of CaCO₃ whiskers can be added to improve various properties. The different content of the three admixtures has different improvement on the each property. The appropriate content should be selected according to the performance requirements and priorities.

Declaration of competing interest

The authors declare that they have no known competing financial interests or personal relationships that could have appeared to influence the work reported in this paper.

Acknowledgements

This work was supported by the National Natural Science Foundation of China [grant numbers U1906229]; the National Natural Science Foundation of China [grant numbers 52109128]; the Natural Science Foundation of Shandong Province [grant numbers ZR2020QE291] and the National Key Research and Development Program [grant numbers 2019YFC1805402].

REFERENCES

- [1] Zhou Z, Wang C, Han X. Safety evaluation of cracked concrete structures with crack length index. *Theor Appl Fract Mech* 2022;122:103662. <https://doi.org/10.1016/j.tafmec.2022.103662>.
- [2] Song L, Sun H, Liu J, Yu Z, Cui C. Automatic segmentation and quantification of global cracks in concrete structures based on deep learning. *Measurement* 2022;199:111550. <https://doi.org/10.1016/j.measurement.2022.111550>.
- [3] Liu B, Shi J, Sun M, He Z, Xu H, Tan J. Mechanical and permeability properties of polymer-modified concrete using hydrophobic agent. *J Build Eng* 2020;31:101337. <https://doi.org/10.1016/j.jobe.2020.101337>.
- [4] Li G, Ding Y, Gao T, Qin Y, Lv Y, Wang K. Chloride resistance of concrete containing nanoparticle-modified polymer cementitious coatings. *Construct Build Mater* 2021;299:123736. <https://doi.org/10.1016/j.conbuildmat.2021.123736>.
- [5] Li G, Bai Z, Zhang G, Wu Y. Study on properties and degradation mechanism of calcium sulfoaluminate cement - ordinary Portland cement binary repair material under seawater erosion. *Case Stud Constr Mater* 2022;17:e01440. <https://doi.org/10.1016/j.cscm.2022.e01440>.
- [6] Shi C, Zou X, Yang L, Wang P, Niu M. Influence of humidity on the mechanical properties of polymer-modified cement-based repair materials. *Construct Build Mater* 2020;261:119928. <https://doi.org/10.1016/j.conbuildmat.2020.119928>.
- [7] Liu C, Huang X, Wu Y, Deng X, Zheng Z. The effect of graphene oxide on the mechanical properties, impermeability and corrosion resistance of cement mortar containing mineral admixtures. *Construct Build Mater* 2021;288:123059. <https://doi.org/10.1016/j.conbuildmat.2021.123059>.
- [8] Zhang C, Lu R, Guan Y, Li X. Effect of crystalline admixtures on mechanical, self-healing and transport properties of engineered cementitious composite. *Cement Concr Compos* 2021;124:104256. <https://doi.org/10.1016/j.cemconcomp.2021.104256>.
- [9] Fu Q, Xu W, Bu M, Guo B, Niu D. Orthogonal experimental study on hybrid-fiber high-durability concrete for marine environment. *J Mater Res Technol* 2021;13:1790–804. <https://doi.org/10.1016/j.jmrt.2021.05.088>.
- [10] Zhang X, Du M, Fang H, Shi M, Zhang C, Wang F. Polymer-modified cement mortars: their enhanced properties, applications, prospects, and challenges. *Construct Build Mater* 2021;299:124290. <https://doi.org/10.1016/j.conbuildmat.2021.124290>.
- [11] Saulat H, Cao M, Khan MM, Khan M, Khan MM, Rehman A. Preparation and applications of calcium carbonate whisker with a special focus on construction materials. *Construct Build Mater* 2020;236:117613. <https://doi.org/10.1016/j.conbuildmat.2019.117613>.
- [12] Althoe F, Zaid O, Martinez-Garcia R, Alsharari F, Ahmed M, Arbili MM. Impact of Nano-silica on the hydration, strength, durability, and microstructural properties of concrete: a state-of-the-art review. *Case Stud. Constr. Mat.* 2023;18:e01997. <https://doi.org/10.1016/j.cscm.2023.e01997>.
- [13] Aggarwal LK, Thapliyal PC, Karade SR. Properties of polymer-modified mortars using epoxy and acrylic emulsions. *Construct Build Mater* 2007;21:379–83. <https://doi.org/10.1016/j.conbuildmat.2005.08.007>.
- [14] Costas and T. Minas AA. Experimental data on the properties of polymer-modified cement grouts using epoxy and acrylic resin emulsions. *Data Brief* 2016;9:463–9. <https://doi.org/10.1016/j.dib.2016.09.016>.
- [15] Cheng J, Shi X, Xu L, Zhang P, Zhu Z, Lu S, et al. Investigation of the effects of styrene acrylate emulsion and vinyl acetate ethylene copolymer emulsion on the performance and microstructure of mortar. *J Build Eng* 2023;75:106965. <https://doi.org/10.1016/j.jobe.2023.106965>.
- [16] Shirshova N, Menner A, Funkhouser GP, Bismarck A. Polymerised high internal phase emulsion cement hybrids: macroporous polymer scaffolds for setting cements. *Cement Concr Res* 2011;41:443–50. <https://doi.org/10.1016/j.cemconres.2011.01.017>.
- [17] Gao Y, Luo J, Yuan S, Zhang J, Gao S, Zhu M, et al. Fabrication of graphene oxide/fiber reinforced polymer cement mortar with remarkable repair and bonding properties. *J Mater Res Technol* 2023;24:9413–33. <https://doi.org/10.1016/j.jmrt.2023.05.144>.
- [18] Yu P, Guorong Z, Yuxuan Q, Qiang Z. In-situ assessment of the water-penetration resistance of polymer modified cement mortars by XCT, SEM and EDS. *Cement Concr Compos* 2020;114:103821. <https://doi.org/10.1016/j.cemconcomp.2020.103821>.
- [19] Pang B, Jia Y, Pang SD, Zhang Y, Du H, Geng G, et al. The interpenetration polymer network in a cement paste - waterborne epoxy system. *Cement Concr Res* 2021;139:106236. <https://doi.org/10.1016/j.cemconres.2020.106236>.
- [20] Chen H, Ma C, Zhang H, Yin Y. Study on skid resistance and skid - resistance durability of polymer modified cement mortar based on surface texture properties. *Construct Build Mater* 2023;370:130645. <https://doi.org/10.1016/j.conbuildmat.2023.130645>.
- [21] Jo Y. Adhesion in tension of polymer cement mortar by curing conditions using polymer dispersions as cement

- modifier. *Construct Build Mater* 2020;242:118134. <https://doi.org/10.1016/j.conbuildmat.2020.118134>.
- [22] Xie C, Cao M, Si W, Khan M. Experimental evaluation on fiber distribution characteristics and mechanical properties of calcium carbonate whisker modified hybrid fibers reinforced cementitious composites. *Construct Build Mater* 2020;265:120292. <https://doi.org/10.1016/j.conbuildmat.2020.120292>.
- [23] Li L, Cao M, Yin H. Comparative roles between aragonite and calcite calcium carbonate whiskers in the hydration and strength of cement paste. *Cement Concr Compos* 2019;104:103350. <https://doi.org/10.1016/j.cemconcomp.2019.103350>.
- [24] Li M, Liu M, Yang YY, Li ZY, Guo XY. Mechanical properties of oil well cement stone reinforced with hybrid fiber of calcium carbonate whisker and carbon fiber. *Petrol Explor Dev* 2015;42:104–11. [https://doi.org/10.1016/S1876-3804\(15\)60012-X](https://doi.org/10.1016/S1876-3804(15)60012-X).
- [25] Yuan Z, Zhang C, Xia C, Wu L, Yu Z, Li Z. Flexural properties of PVA fiber reinforced high ductility cementitious composites containing calcium carbonate whisker. *Construct Build Mater* 2021;300:124329. <https://doi.org/10.1016/j.conbuildmat.2021.124329>.
- [26] Xie C, Cao M, Yin H, Guan J, Wang L. Effects of freeze-thaw damage on fracture properties and microstructure of hybrid fibers reinforced cementitious composites containing calcium carbonate whisker. *Construct Build Mater* 2021;300:123872. <https://doi.org/10.1016/j.conbuildmat.2021.123872>.
- [27] Cao M, Liu Z, Xie C. Effectiveness of calcium carbonate whiskers in mortar for improving the abrasion resistance. *Construct Build Mater* 2021;295:123583. <https://doi.org/10.1016/j.conbuildmat.2021.123583>.
- [28] Zhang J, Jin J, Guo B, Wang J, Fu C, Zhang Y. Effect of mixed basalt fiber and calcium sulfate whisker on chloride permeability of concrete. *J Build Eng* 2023;64:105633. <https://doi.org/10.1016/j.jobe.2022.105633>.
- [29] Vijayan DS, Devarajan P, Sivasuriyan A. A review on eminent application and performance of nano based silica and silica fume in the cement concrete. *Sustain Energy Techn* 2023;56:103105. <https://doi.org/10.1016/j.seta.2023.103105>.
- [30] Kooshafar M, Madani H. An investigation on the influence of nano silica morphology on the characteristics of cement composites. *J Build Eng* 2020;30:101293. <https://doi.org/10.1016/j.jobe.2020.101293>.
- [31] Zhang G, Xia H, Niu Y, Song L, Zhao Y, Lv X, et al. Microstructure refinement and affected zone reinforcement for internal curing cement paste by composite microgel with nano silica. *Cement Concr Compos* 2023;138:105013. <https://doi.org/10.1016/j.cemconcomp.2023.105013>.
- [32] Hamza Güllü MEYE. Effect of using nano-silica on the rheological, fresh and strength characteristics of cement-based grout for grouting columns. *J Build Eng* 2023;76:107100. <https://doi.org/10.1016/j.jobe.2023.107100>.
- [33] Benkirane O, Haruna S, Fall M. Strength and microstructure of cemented paste backfill modified with nano-silica particles and cured under non-isothermal conditions. *Powder Technol* 2023;419:118311. <https://doi.org/10.1016/j.powtec.2023.118311>.
- [34] Liu X, Liu R, Xie X, Zuo J, Lyu K, Shah SP. Chloride corrosion resistance of cement mortar with recycled concrete powder modified by nano-silica. *Construct Build Mater* 2023;364:129907. <https://doi.org/10.1016/j.conbuildmat.2022.129907>.
- [35] Bai S, Yu L, Guan X, Li H, Ou J. Study on the long-term chloride permeability of nano-silica modified cement pastes cured at negative temperature. *J Build Eng* 2022;57:104854. <https://doi.org/10.1016/j.jobe.2022.104854>.
- [36] Xu J, Li Y, Lu L, Cheng X, Li L. Strength and durability of marine cement-based mortar modified by colloidal nano-silica with epoxy silane for low CO₂ emission. *J Clean Prod* 2023;382:135281. <https://doi.org/10.1016/j.jclepro.2022.135281>.
- [37] Lu C, Zhang Z, Shi C, Li N, Jiao D, Yuan Q. Rheology of alkali-activated materials: a review. *Cement Concr Compos* 2021;121:104061. <https://doi.org/10.1016/j.cemconcomp.2021.104061>.
- [38] Han F, Pu S, Zhou Y, Zhang H, Zhang Z. Effect of ultrafine mineral admixtures on the rheological properties of fresh cement paste: a review. *J Build Eng* 2022;51:104313. <https://doi.org/10.1016/j.jobe.2022.104313>.
- [39] Zhaidarbek B, Tleubek A, Berdibek G, Wang Y. Analytical predictions of concrete pumping: extending the Khatib-Khayat model to Herschel-Bulkley and modified Bingham fluids. *Cement Concr Res* 2023;163:107035. <https://doi.org/10.1016/j.cemconres.2022.107035>.
- [40] Wang Z, Guo W, Ding W, Liu K, Qin W, Wang C, et al. Numerical study on the hydrodynamic properties of bentonite slurries with Herschel-Bulkley-Papanastasiou rheology model. *Powder Technol* 2023;419:118375. <https://doi.org/10.1016/j.powtec.2023.118375>.
- [41] Guo Y, Ma B, Zhi Z, Tan H, Liu M, Jian S, et al. Effect of polyacrylic acid emulsion on fluidity of cement paste. *Colloid Surface* 2017;535:139–48. <https://doi.org/10.1016/j.colsurfa.2017.09.039>.
- [42] Ouyang J, Han B, Cao Y, Zhou W, Li W, Shah SP. The role and interaction of superplasticizer and emulsifier in fresh cement asphalt emulsion paste through rheology study. *Construct Build Mater* 2016;125:643–53. <https://doi.org/10.1016/j.conbuildmat.2016.08.085>.
- [43] Cao M, Xu L, Zhang C. Rheology, fiber distribution and mechanical properties of calcium carbonate (CaCO₃) whisker reinforced cement mortar. *Compos Part a-Appl S* 2016;90:662–9. <https://doi.org/10.1016/j.compositesa.2016.08.033>.
- [44] Roshani A, Fall M. Rheological properties of cemented paste backfill with nano-silica: link to curing temperature. *Cement Concr Compos* 2020;114:103785. <https://doi.org/10.1016/j.cemconcomp.2020.103785>.
- [45] Bai S, Guan X, Li H, Ou J. Effect of the specific surface area of nano-silica particle on the properties of cement paste. *Powder Technol* 2021;392:680–9. <https://doi.org/10.1016/j.powtec.2021.07.045>.
- [46] Liu B, Zhou H, Meng H, Pan G, Li D. Fresh properties, rheological behavior and structural evolution of cement pastes optimized using highly dispersed in situ controllably grown Nano-SiO₂. *Cement Concr Compos* 2023;135:104828. <https://doi.org/10.1016/j.cemconcomp.2022.104828>.
- [47] Shirshova N, Menner A, Funkhouser GP, Bismarck A. Polymerised high internal phase emulsion cement hybrids: macroporous polymer scaffolds for setting cements. *Cement Concr Res* 2011;41:443–50. <https://doi.org/10.1016/j.cemconres.2011.01.017>.
- [48] Cao M, Ming X, Yin H, Li L. Influence of high temperature on strength, ultrasonic velocity and mass loss of calcium carbonate whisker reinforced cement paste. *Compos. Part B-Eng* 2019;163:438–46. <https://doi.org/10.1016/j.compositesb.2019.01.030>.
- [49] Mohammed Arif SDHS. Effect of nano silica on strength and permeability of concrete. *Mater Today Proc* 2023. <https://doi.org/10.1016/j.matpr.2023.04.073>.
- [50] Ferdous W, Manalo A, Wong HS, Abousnina R, AlAjarmeh OS, Yan ZG, et al. Optimal design for epoxy polymer concrete based on mechanical properties and durability aspects. *Construct Build Mater* 2020;232:117229. <https://doi.org/10.1016/j.conbuildmat.2019.117229>.

- [51] Tran NP, Nguyen TN, Ngo TD. The role of organic polymer modifiers in cementitious systems towards durable and resilient infrastructures: a systematic review. *Construct Build Mater* 2022;360:129562. <https://doi.org/10.1016/j.conbuildmat.2022.129562>.
- [52] Wang J, Ma L, Lu L, Fu Q, Li X, Zhang R, et al. Improving the wear resistance and chloride permeability of sulphoaluminate cement by spindle-like calcium carbonate modification. *Mater Today Commun* 2022;32:104037. <https://doi.org/10.1016/j.mtcomm.2022.104037>.
- [53] Tabish M, Zaheer MM, Baqi A. Effect of nano-silica on mechanical, microstructural and durability properties of cement-based materials: a review. *J Build Eng* 2023;65:105676. <https://doi.org/10.1016/j.jobe.2022.105676>.
- [54] Praveen KVV, Dey S. Study on strength and durability characteristics of nano-silica based blended concrete. *Hybrid Advances* 2023;2:100011. <https://doi.org/10.1016/j.hybadv.2022.100011>.
- [55] Liu Y, Wang J, Hu S, Cao S, Wang F. Enhancing the mechanical behaviour of concretes through polymer modification of the aggregate-cement paste interface. *J Build Eng* 2022;54:104605. <https://doi.org/10.1016/j.jobe.2022.104605>.
- [56] Ramli M, Tabassi AA. Effects of polymer modification on the permeability of cement mortars under different curing conditions: a correlational study that includes pore distributions, water absorption and compressive strength. *Construct Build Mater* 2012;28:561–70. <https://doi.org/10.1016/j.conbuildmat.2011.09.004>.